Numerical Investigation on Frictional Pressure Loss in a Perfect Square Micro Channel with Roughness and Particles

Donghyouck Han
Research Institute of Engineering & Technology, Korea University, Seoul 136-701, Korea
Kyu-Jung Lee*
Department of Mechanical Engineering, Korea University, Seoul, 136-701, Korea

A numerical study is performed to investigate the effect of inner surface roughness and micro-particles on adiabatic single phase frictional pressure drop in a perfect square micro channel. With the variation of particles sizes (0.1 to 1 μm) and occupied volume ratio (0.01 to 10%) by particles, the Eulerian multi-phase model is applied to a 100 μm hydraulic diameter perfect square micro channel in laminar flow region. Frictional pressure loss is affected significantly by particle size than occupied volume ratio by particles. The particle properties like density and coefficient of restitution are investigated with various particle materials and the density of particle is found as an influential factor. Roughness effect on pressure drop in the micro channel is investigated with the consideration of roughness height, pitch, and distribution. Additionally, the combination effect by particles and surface roughness are simulated. The pressure loss in microchannel with 2.5% relative roughness surface can be increased more than 20% by the addition of 0.5 μm diameter particles.

Key Words: Microfluidics, Pressure Drop, Numerical Simulation, Friction Factor, MEMS, Roughness, Nano-Particle

Nomenclature

A_D : Parameter for drag force [kg/m^{3}s]
C_D : Drag coefficient [dimensionless]
d : Dispersed phase mean diameter [m]
D_h : Hydraulic diameter [m]
e : roughness height [m] or restitution coefficient [dimensionless]
F_{int} : Internal force [N/m^3]
g : Gravity vector [m/s^2]
g_o : Radial distribution [dimensionless]
M : Inter-phase momentum transfer per unit volume [N/m^3]
p : Pressure [N/m^2]
Re : Reynolds number [dimensionless]
Re_e : Roughness Reynolds number [dimensionless]
u : Mean phase velocity [m/s]

Greek letters

α : Volume fraction [dimensionless]
Δ : Difference [dimensionless]
μ : Shear viscosity [Ns/m^2]
ν_t : Turbulent kinematic viscosity [m^2/s]
Θ : Granular temperature [m^2/s^2]
ρ : Density [kg/m^3]
σ_α : Turbulent Prandtl number [dimensionless]
τ : Stress [N/m^2]
ξ : Bulk viscosity [Ns/m^2]

Subscript

c : Continuous phase
d : Particle

* Corresponding Author,
E-mail : kjlee@korea.ac.kr
TEL : +82-2-3290-3359; **FAX** : +82-2-928-9768
Department of Mechanical Engineering, Korea University, Seoul, 136-701, Korea. (Manuscript **Received** December 13, 2005; **Revised** May 4, 2006)

k : Phase
r : Relative
s : Solid

1. Introduction

With the increase of interest in micro-devices, it is highly required to understand the fluid physics in micro tubes. Although a lot of researchers have been devoted for the pressure loss measurements in micro channels, discrepancies among the previous experimental results still exist. Kedzierski (2003) reviewed previous results that showed the discrepancy between macro prediction method and the experimental results in microchannels and indicated several micro-effects like velocity slip, temperature jump, viscous dissipation, developing flow, eddy bursting, size dependent viscosity, roughness, compressibility, and flow mal-distribution. Mala and Li (1999) suggested that surface roughness contributed to the early transition from laminar to turbulent flow. Brutin and Tadrist (2003) carried out experiments in micro-channels with deactivated and non-deactivated surfaces. They reported that the polarity of the surface is influential on pressure loss in micro channels. Ghiaasiaan and Laker (2001) suggested that suspended microscopic particles might be a major contributor to the inconsistencies and disagreements in the published data. Xu et al.(2003) proposed a criterion to draw the limit of the significance of the viscous dissipation effects theoretically.

Generally, an experiment can be affected by several different causes at the same time and it is difficult to estimate the relationship between considered cause and flow characteristic. Thus, numerical approach is needed to understand the effect of each isolated cause. In this numerical study, adiabatic pressure loss in a perfect square micro channel with the consideration of micro-particles and inner surface roughness were obtained with the aid of conventional finite volume method software. As stated above, other microscopic effects as Kedzierski (2003) indicated were not taken into account and numerical models were solved in incompressible flow condition in laminar flow region.

2. Numeircal Method

In all simulations, water properties at 298.15 K were used and an incompressible flow and an adiabatic condition were assumed. Because of the numerical reliability of transitional region from laminar to turbulent flow, this study was restricted to the laminar flow region. Actually, it is quite difficult to achieve turbulent flow because of extremely high pressure loss in microchannels. The governing equations were solved numerically using commercial FVM (finite volume method) software STAR-CD (2004). STAR-CD simultaneously solves the momentum, continuity, and energy equations by means of the control volume based technique. The SIMPLE algorithm was adopted and convergence is declared as the normalized residual are less than 10^{-4}.

A periodic inlet/outlet and a symmetry boundary condition were introduced to save computing time. Periodic condition was applied to inlet and outlet boundaries to obtain fully developed flow condition. Because of the symmetry plane at the center of channel, only 25% of total cross section was used in this simulation. Fig. 1 shows the considered structure. It has 50 μm×50 μm×90 μm (x×y×z) dimensions. Grid spacing was increased toward the wall. Grid dependence of the results was examined by using different mesh sizes. Finally, a grid with 360,000 cells was chosen.

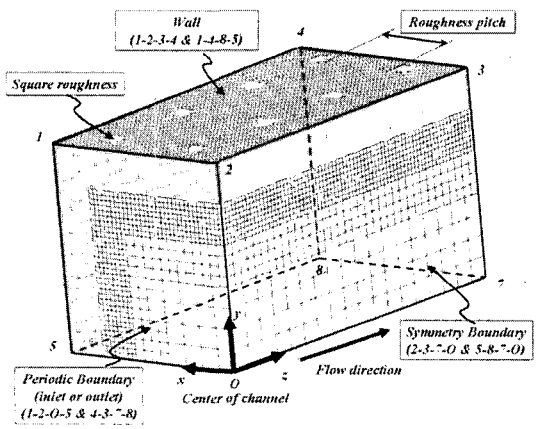

Fig. 1 Mesh structure

2.1 Roughness effect

Square blocks were attached on inner wall to simulate rough surface. The block shape was intended for the maximization of pressure loss. A similar geometry was also used for the investigation of particles effect. Square blocks were distributed uniformly or randomly as specific surface condition. Figures 1 and 2 show a rough surface with uniformly distributed blocks. Figure 3 shows blocks with random heights. In this case, average roughness height was used to determine roughness pitch. Uniformly distributed rough surface means an inner wall has a uniform roughness distribution along flow direction and perimeter with a fixed roughness pitch. The roughness pitch was defined as the ratio between the height of square block and distance between square blocks. Inner walls with random roughness distribution were shown in Figure 4(a) and 4(b). In this study, two different random roughness distributions were investigated. Figures 2 and 3 show velocity profile as roughness distribution. From the difference between Figures 2 and 3, it can be found that the investigation of the effect of roughness distribution is needed.

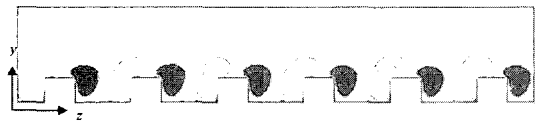

Fig. 2(a) u velocity contour on yz plane with uniform roughness height and pitch

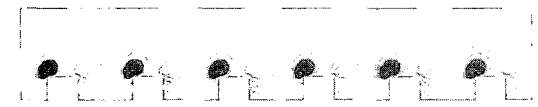

Fig. 2(b) v velocity contour on yz plane with uniform roughness height and pitch

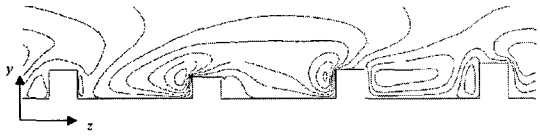

Fig. 3(a) u velocity contour on yz plane with non-uniform roughness height and uniform pitch

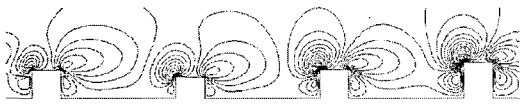

Fig. 3(b) v velocity contour on yz plane with non-uniform roughness height and uniform pitch

2.2 Particle effect

To investigate the micro-particle effect on pressure loss in micro-channel, the Eulerian multi-phase model (Bracco, 1985) was adopted. In the Eulerian multi-phase model, the phases are treated as interpenetrating continua coexisting in the flow domain. Equations for conservation of mass, momentum and energy are solved for each phase. The share of the flow domain occupied by each phase is given by its volume fraction and each phase has its own velocity, temperature and physical properties. Interactions between phases due to differences in velocity and temperature are taken into account via the inter-phase transfer terms in the transport equations.

The continuity and momentum equations for the Eulerian two-phase models are

$$\frac{\partial}{\partial t}(\alpha_k\rho_k)+\nabla\cdot(\alpha_k\rho_k u_k)=0 \tag{1}$$

where, α_k, ρ_k, and u_k are volume fraction, density and mean phase velocity, respectively.

$$\frac{\partial}{\partial t}(\alpha_k\rho_k u_k)+\nabla\cdot(\alpha_k\rho_k u_k u_k) = -\alpha_k\nabla p+\alpha_k\rho_k g+\nabla\cdot(\alpha_k\tau_k)+M_k+(F_{\mathrm{int}})_k \tag{2}$$

where, τ_k, p, M_k, $(F_{int})_k$, and g are molecular stress, pressure (assumed to be equal in both phases), inter-phase momentum transfer per unit volume, internal forces, and gravity vector, respectively.

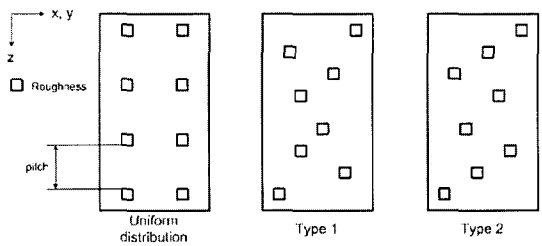

Fig. 4 Surface roughness distribution

The inter-phase momentum transfer represents the sum of all the forces the phases exert on one another and satisfies $M_c=-M_d$. The internal forces represent forces within a phase. Particle-particle interactions can be very significant in solid particle flows and they require their own set of models. In this analysis, kinetic theory stress tensor model was applied.

By analogy with the gas kinetic theory, and after assuming distribution and collision properties for the particles, a kinetic theory of granular flows can be derived. A full stress tensor is then obtained that describes the particle-particle interaction terms in the solid phase momentum equation:

$$(F_{\text{int}})_d=\nabla\cdot\bar{S}_s \tag{3}$$

where the granular stress tensor is defined as

$$S_s=\left[-P_s+\left(\bar{\xi}_s-\frac{2}{3}\mu_s\right)\nabla\cdot u_d\right]I \tag{4}$$

and P_s, ξ_s, and μ_s are solid pressure, solid phase bulk viscosity, and solid phase shear viscosity, respectively.

Expressions for the solid pressure, bulk, and shear viscosities are obtained as functions of the solid granular temperature, Θ.

The solid pressure is

$$P_s=\alpha_d\rho_d\Theta[1+2(1+e)g_o\alpha_d] \tag{5}$$

the solid-phase bulk viscosity

$$\xi_s=\frac{4}{3}\alpha_d^2\rho_d d g_o(1+e)\sqrt{\frac{\Theta}{\pi}} \tag{6}$$

and the solid-phase shear viscosity is

$$\mu_s=\frac{2\mu_{s,dil}}{(1+e)g_o}\left[1+\frac{4}{5}(1+e)g_o\alpha_d\right]^2+\frac{4}{5}\alpha_d^2\rho_d d g_o(1+e)\sqrt{\frac{\Theta}{\pi}} \tag{7a}$$

$$u_{s,dil}=\frac{5\sqrt{\pi}}{96}\rho_d d\sqrt{\Theta} \tag{7b}$$

where, e and g_o are restitution coefficient and radial distribution. In the kinetic theory of granular flow, Θ is obtained by solving the conservation equation for fluctuating energy.

The restitution coefficient provides a measure of the elasticity of the particles and the amount of energy absorbed in collisions. For copper, e is 0.22.

The radial distribution function represents the spatial distribution of the particles, and therefore their proximity, and can be related to the dispersed-phase volume fraction. The form given by Ding and Gidaspow (1990) has been implemented.

$$g_o=\frac{3}{5}\left[1-\left(\frac{\alpha_d}{\alpha_{d,\max}}\right)^{1/3}\right]^{-1} \tag{8}$$

This function becomes undefined when α_d approaches the maximum packing density $\alpha_{d,\max}$. In this limit, following equation is supplemented by the equation proposed by van Wachem et al. (1998) for $\alpha_d>\alpha_{crit}$.

$$g_o=1.08\times10^3+1.08\times10^6(\alpha_d-\alpha_{crit})+1.08\times10^9(\alpha_d-\alpha_{crit})^2+1.08\times10^{12}(\alpha_d-\alpha_{crit})^3 \tag{9}$$

where $\alpha_{crit}=\alpha_{d,\max}-0.001$.

The momentum transfer term includes the drag, virtual mass and lift forces. The virtual mass force can be neglected if the particles are not accelerated and they follow streamlines in laminar flow. Because the lift force consideration increase pressure drop very slightly but demands computing time much more, its effect was neglected.

The inter-phase drag force includes a mean and a fluctuating component, of which the latter accounts for the additional drag due to interaction between the dispersed phase and the surrounding turbulent eddies. In general form, following the derivation of Gosman et al. (1992), the drag force is modeled as

$$F_D=A_D u_r-A_D\frac{v_c^t}{\alpha_d\alpha_c\sigma_r}\nabla\alpha_d \tag{11}$$

where

$$A_D=\frac{3}{4}\frac{\alpha_d\rho_c C_D}{d}|u_r| \tag{12}$$

And $u_r=u_c-u_d$ is relative velocity between the phases. C_D, d, σ_α and v_c^t are drag coefficient, dispersed phase mean diameter, turbulent Prandtl number, and continuous phase turbulent kinematic viscosity, respectively. With this formulation, the drag force is then fully defined after a model has been chosen for C_D.

The drag coefficient of spherical, rigid particles is computed based on the correlation of Schiller and Naumann (1933).

$$C_D=\frac{24}{\mathrm{Re}_d}(1+0.15\mathrm{Re}_d^{0.687}) \quad : 0<\mathrm{Re}_d\leq 1000 \quad (13a)$$

$$C_D=0.44 \quad : \mathrm{Re}_d>100 \quad (13b)$$

The particle Reynolds number is defined as

$$\mathrm{Re}_d=\frac{\rho_c|u_r|d}{\mu_c} \quad (14)$$

This correlation is generally suitable for spherical solid particles, liquid droplets and small-diameter bubbles.

Properties of water and particles at 298.15 K were used. There is no heat transfer between two phases. Additional information for Eulerian multiphase model can be found in the references (CD Adapco Group, 2004; Bracco, 1985).

3. Results

Pressure loss was investigated in terms of friction factor, C_D, Re, and Re_e. These non-dimensional parameters are defined as follows:

$$\mathrm{Re}=\frac{\rho u D_h}{\mu} \quad (15)$$

$$C_D=\frac{\Delta\rho D_h}{2\rho u^2} \quad (16)$$

$$\mathrm{Re}_e=\mathrm{Re}\left(\frac{e}{D_h}\right)\sqrt{\frac{C_D}{2}} \quad (17)$$

where, u is the average velocity in a channel cross section, ρ is the density of working fluid, D_h is hydraulic diameter, and μ is viscosity.

The simulations were verified to ensure the validity of the numerical analysis. The considered geometry was tested with incompressible water without surface roughness and micro-particles. For the fully developed flow in a perfect square channel, Shah and London (1978) suggested C_D Re is 14.23. Although this reference value came from macro prediction methods, Lelea et al.(2004) reported that macro theory matched well with their own experimental data in micro-channels. And they also reported a lot of similar results according to their review. Therefore, the macro prediction value was used as reference in this numerical study. As the simulation results of the micro channel at Re 500, 400, 300, and 200 were compared to the reference value, 14.23, they showed 1.5, 0.1, 1.7, and 3.7% relative differences, respectively. Therefore, these comparison results show the reliability of this numerical study.

3.1 Roughness effect

Figure 5 shows the effect of roughness pitch on pressure loss. These values were obtained with 5 μm roughness height at Re 500. At a specific roughness pitch, square blocks that were used as roughness were distributed along flow direction and perimeter uniformly. Pressure drop increased with decreasing pitch as indicated in Figure 5. Similar trend was also appeared in the simulation results of Rawool et al.(2005). They used a 100 μm×100 μm diameter channel with 10% relative roughness. Roughness shape was triangular and Re was fixed as 100. Generally, cheap stainless steel micro channels have 5 μm roughness height. At this extreme surface condition (5% relative roughness and roughness pitch=2), Re_ε does not exceed five at Re=500. Corresponding u and v velocity contours on yz plain to this flow condition are shown in Fig. 2(a) and (b),

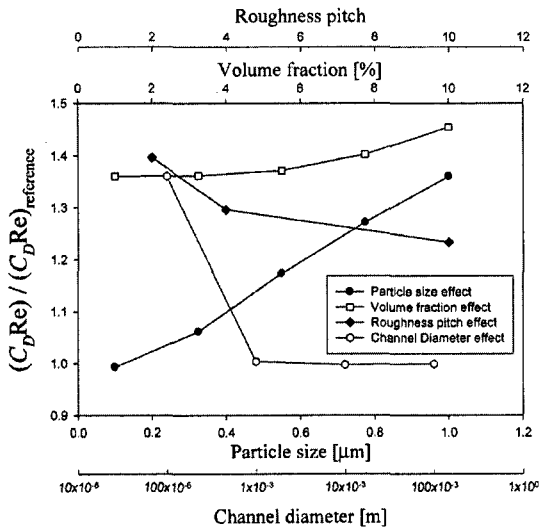

Fig. 5 The effect of roughness pitch, volume fraction, particle size, and diameter

respectively. Because the geometry has a uniform roughness height and a pitch, the same velocity contour is appeared repeatedly.

Table 1 shows the effect of roughness height and Re. From the results of case 3 and 6, roughness height effect can be found clearly. Case 3 gives a hint for a criterion about a minimum roughness height that can influence on pressure drop in the micro channel. It seems that roughness effect on pressure loss up to 2.5 μm roughness height in the considered micro channel (perfect square channel with 100 μm hydraulic diameter) is negligible as the consideration of previous researchers' experimental uncertainties (about 10%). However, the influence of roughness is noticeable for 5% relative roughness surface conditions (case 1 and 6). Case 1 and 2 show flow rate (Re) effect on pressure loss. With increasing Re, pressure drop increases at the same geometric condition because viscous sublayer thickness is getting smaller. At Re was 1000, roughness Re exceeded 5. Therefore, square blocks in this specific geometry (case 2) may disturb laminar sublayer and increase pressure loss. Rawool et al.'s (2005) simulation results showed the increase in pressure loss is non-linear with roughness height regardless of roughness shape. The slope of pressure loss as roughness height increased rapidly with roughness height. This is due to the decrease in flow area with the corresponding increase in velocity. Mala and Li (1999) tested 50-250 μm diameter stainless steel and fused silica tubes with 1.75 μm mean surface roughness. Their 130 μm diameter stainless steel tube showed 60% larger pressure loss than that of macro theory. This relatively large difference might come from their pressure loss calculation procedure. They used two different length tubes with similar tube diameter to remove the effect of developing region and port. According to their tube specification, maximum diameter difference between two similar microtubes is 4 μm. This difference can induce more than 20% higher/lower friction factor in a 100 μm diameter micro-channel. Moreover, it is very difficult to match identical operating temperature and Re because of viscous dissipation and other delicate experimental control problems. They also reported that early transition occurred at Re was 500. They ascribed this early phenomenon to surface roughness. Their transition Re is smaller than that can be inferred from this simulation result. Contrary to Mala and Li (1999), Liu and Garimella (2004) suggested that no early transition occurred for their micro channels. Their micro-channels had less than 3% relative roughness and the channels were rectangular. Their frictional loss agreed well with the conventional macro theory. Even though the hydraulic diameters of theirs were larger (244~974 μm) than that of this simulation model (100 μm), it seems that the result of case 3 in Table 1 (relative roughness=2.5%) agrees with the experimental result of Liu and Garimella (2004).

Table 1 The effect of roughness height, Re, pitch, and volume ratio

Case	Re	e [μm]	pitch	d [μm]	α [%]	$(C_D Re)/(C_D Re)_{reference}$	Roughness type*
1	500	5	2	N/A	N/A	1.38	UH & UD
2	1000	5	2	N/A	N/A	1.45	UH & UD
3	500	2.5	4	N/A	N/A	1.13	UH & UD
4	500	2.5	4	0.5	0.1	1.42	UH & UD
5	500	2.5	4	0.5	0.01	1.38	UH & UD
6	500	5	4	N/A	N/A	1.30	UH & UD
7	500	5	4	N/A	N/A	1.32	RH & UD
8	500	5	N/A	N/A	N/A	1.32	UH & RD (Type 1)
9	500	5	N/A	N/A	N/A	1.33	UH & RD (Type 2)

*Notice
UH : uniform height UD : uniform distribution
RH : random height RD : random distribution

This numerical result shows slightly higher pressure loss than the measurements of Liu and Garimeall (2004). It may be induced by adopting square block roughness shape and small roughness pitch (2) for the simulation geometry. Actually, it is extremely difficult to model the real surface of microchannels. Therefore, careful investigations and approaches are needed to ascribe early transition phenomenon and increased pressure in microchannels to roughness effect.

Real surfaces of microchannels have random roughness distribution. According to Croce and D'Agaro (2004), a surface that has random roughness distribution increased about 6% higher pressure loss than that of one has uniform roughness distribution. Case 6, 7, 8, and 9 shows the effect of roughness distribution and irregular height. For case 7, 5, 3.75, and 6.25 μm roughness heights were randomly distributed on inner surface. Typical velocity contours are shown in Fig. 3. Case 8 and 9 adopted roughness distributions in Figure 4. Although random roughness distribution increased pressure loss, the augmented values were very small. These results can be explained with the concept of roughness Re. Under this flow and surface condition, roughness Re exceeded five barely. Most of square blocks were placed beneath viscous sublayer. Therefore, the effect of roughness distribution and geometry may not be appeared considerably. If random roughness distribution and roughness height are introduced at the same time, their combination effect may increase pressure loss as much as 6% that was reported by Croce and D'Agaro (2004).

3.2 Particle effect

Figure 5 shows the importance of micro-particle effect on pressure loss in micro-channels. As the volume ratio between copper particles and water was 1% and particle size was 1 μm, micro-particles did not affect pressure loss up to millimeter scale at Re was 500. Xuan and Li (2003) measured the turbulent friction factor of water-based nanofluids containing Cu nanoparticles in a volume fraction range of 1.0-2.0. The test tube had 10 mm diameter. Like this simulation results, they found that the friction factor for the nanofluids was approximately the same as that of water. The viscosity of fluids with micro/nano particles depends on the methods used to disperse and stabilize the particle suspension. In this case, properties are very similar to those of the base fluid because of low volume fraction. However, for the 100 μm hydraulic diameter perfect square channel at Re 500, its CDRe was over 30% larger than that of the reference value. Hence, the effect of micro-particle cannot be neglected in micro-channels.

Figure 4 also shows the effect of particle diameter and volume fraction on pressure loss. The effect of micro-particle size was investigated in the range of 0.1 to 1 μm with 1% volume fraction at Re was 500. Copper was used as the particles. Pressure drop increases linearly with particle diameter. Generally, the uncertainties of previous researches were about 10% for single phase pressure drop in micro-channels. Micro-particles over 0.5 μm diameter size with 1% volume ratio increase pressure drop more than 10%. Therefore, previous experimental results using filters that had larger pore than 0.5 μm should be reevaluated with the consideration of the effect by micro-particles. Pressure loss increases slightly with volume ratio. This phenomenon can be explained with the measurements of Liu et al. (2006). They showed the effective viscosity of nanofluids (CuO-

Table 2 The effect of particle properties

Material	Density [kg/m^3]	Coefficient of restitution	$(C_D\mathrm{Re})/(C_D\mathrm{Re})_{\mathrm{reference}}$
Lead	11,370	0.16	1.49
Iron	7,860	0.67	1.23
Copper	8,960	0.22	1.36
Glass	2,600	0.96	1.03
Steel	7,840	0.90	1.21

ethylene glycol) increased with volume fraction (1~5%). However, the effect of volume ratio was not shown distinctively as that of micro-particle size. This phenomenon was also detected in the measurement of Xuan and Li (2003) (volume fraction : 1~2%)

The effect of particle properties was shown in Table 2. The density and the coefficient of restitution were considered in this study. Volume ratio, particle size, and Re were fixed as 1%, 1 μm, and 500, respectively. Although lead has the lowest coefficient of restitution among considered particle materials, its C_DRe is the largest among particles. The comparison result between glass and steel particles that have similar coefficient of restitution shows steel has larger C_DRe value than that of glass even though it has slightly lower coefficient of restitution than that of glass. It seems that the density of particle has more dominant influence on pressure loss than coefficient of restitution. It is also noticeable that particles that have higher densities like metals can increase pressure loss. For glass particles, its C_DRe value is almost same as pure water without particles.

3.3 Combination effect of roughness and particles

The combination effect by inner surface roughness and micro particles were carried out at 100 μm diameter rectangular channel with 2.5 μm roughness height and roughness pitch is 4. Re was fixed as 500. From Table 1 (case 3 and 5), pressure loss in rough surface can be increased about 25% with 0.5 μm diameter particles even if the volume ratio is only 0.01%. Therefore, simultaneous contribution by roughness and particles affects pressure loss in micro channels significantly. Currently, filters that have less than 0.5 μm pore size are available. Hence, careful consideration of proper filtering size is necessary to investigate the characteristics of microfluidic devices.

4. Conclusions

The effect of inner surface roughness and micro particles on single phase adiabatic pressure loss in a perfect square micro channel with 100 μm hydraulic diameter was investigated numerically with the aid of conventional FVM software. The Eulerian multi-phase model was adopted. With varying particle size from 0.1 to 1 μm and volume ratio from 0.01 to 10%, frictional coefficients were obtained. Apparently, inner surface roughness and particles affect on pressure loss in microchannels. If previous researchers' microchannels had problems with roughness and filtering, the discrepancies between macro prediction and their experimental results can be explained with those effects. Therefore, careful consideration of roughness and filter selection is needed to investigate flow characteristics in microfluidic devices.

Acknowledgments

This work was supported by the Korea Research Foundation Grant funded by the Korean Government (MOEHRD). (KRF-2004-214-D00020).

References

Bracco, F. V., 1985, "Modeling of Engine Sprays," SAE Technical Paper Series 850394.

Brutin, D. and Tadrist, L., 2003, "Experimental Friction Factor of a Liquid flow In Microtubes," *Physics of Fluids*, Vol. 15, No. 3, pp. 653~661.

CD Adapco Group, 2004, Methodology, STAR-CD ver. 3.22, CD Adapco, London, Chap. 13, pp. 13.1~13.9.

Croce, G. and D'Agaro, P., 2004, "Numerical Analysis of Roughness Effect on Microtube Heat Transfer," *J. Superlattices and Microstructures*, Vol. 35, pp. 601~616.

Ding, J. and Gidaspow, D., 1990, *Turbulence in Liquid and Phase of a Uniform Bubbly Air-Water Flow*, J. Fluid Mech., Vol. 222, pp. 95-118.

Ghiaasiaan, S. M. and Laker, T. S., 2001, "Turbulent Forced Convection in Microtubes," *Int. J. of Heat and Mass Transfer*, Vol. 44, pp. 2777~2782.

Gosman, A. D., Issa, R. I., Lekakou, C., Looney, M. K. and Politis, S., 1992, *Multidimensional Modelling of Turbulent Two-Phase Flows in Stirred Vessels*, AIChE Journal, Vol. 38, No. 12, pp. 1946~1956.

Kedzierski, M. A., 2003, "Micro Channel Heat Transfer, Pressure Drop And macro Prediction Methods," Keynote for 2nd Int. Conference on Heat Transfer, Fluid Mechanics, and Thermodynamics, June 23-26, Victoria Falls, Zambia

Lelea, D., Nishio, S. and Takano, K., 2004, "The Experimental Research on Microtube Heat Transfer and Fluid Flow of Distilled Water," *Int. J. of Heat and mass Transfer*, Vol. 47, pp. 2817~2830.

Liu, D. and Garimella, S. V., 2004, *Investigation of Liquid Flow in Microchannels*, J. of Thermophysics and Heat transfer, Vol. 18, No. 1, pp. 65~72.

Liu, M. Lin, M. C., Huang, I. and Wang, C., 2006, *Enhancement of Thermal Conductivity with CuO for Nanofluids*, Chem. Eng. Technol., Vol. 29, No. 1, pp. 72~77.

Mala, G. M. and Li, D., 1999, "Flow Characteristics of Water in Microtubes," *Int. J. of Heat and Fluid Flow*, Vol. 20, pp. 142~148.

Rawool, A. S., Sushanta, K., Mitra, S. and Kandlikar G., 2005, *Numerical Simulation of Flow Through Microchannels with Designed Roughness*, Microfluid Nanofluid, Springer-Verlag, DOI 10.1007/s10404-00500064-5.

Schiller, L. and Naumann, A., 1933, "Ber Die Grundlegenden Berechnungen Bei Der Schwerkraftaufbereitung," *VDI Zeits.*, Vol. 77, No. 12, pp. 318~320.

Shah, R. K. and London, A. L, 1978, "Laminar Flow Forced Convection in Ducts," Supplement 1 to Advances in Heat Transfer, eds. Irvine, T.F., Hartnett, J. P., Academic Press, New York.

Xu, B., Ooi, K. T., Mavriplis C. and Zaghloul, M. E., 2003, "Evaluation of Viscous Dissipation in Liquid Flow in Microchannels," *J. Micromech. Microeng*, Vol. 13, pp. 53~57.

Xuan, Y. and Li, Q., 2003, *Investigation on Convective Heat Transfer and Flow Features of Nanofluids*, J. of Heat Transfer, Vol. 125, pp. 151~155.

van Wachem, B., Schouten, J. C., Krishna, R. and van den Bleek, C. M., 1998, "Eulerian Simulations of Bubbling Behaviour in Gas-Solid Fluidized Beds," Computers Chem. Eng., Vol. 22, Supple., pp. S299~S306.